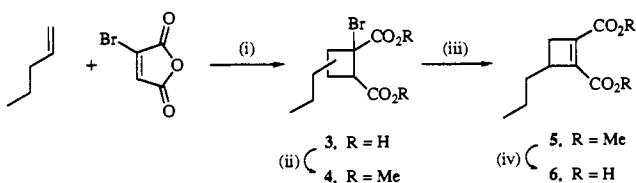
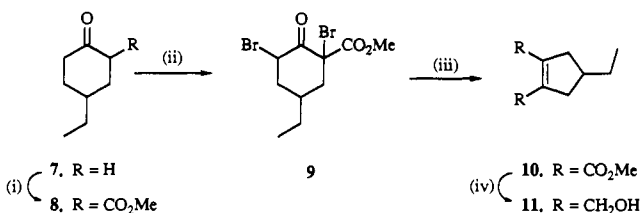
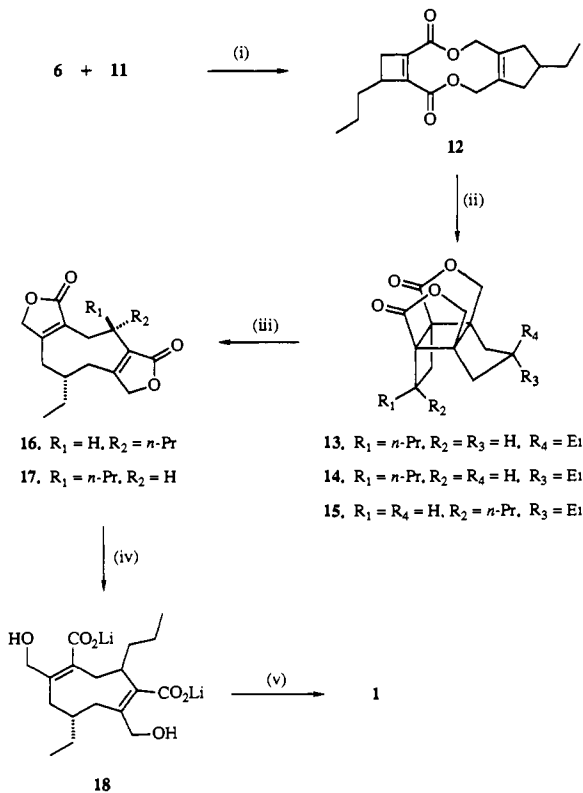


Scheme I<sup>a</sup>

<sup>a</sup> (i)  $h\nu$ ,  $\text{Ph}_2\text{CO}$ ,  $\text{MeCN}$ , then  $\text{Na}_2\text{CO}_3$  (aqueous), then  $\text{HCl}$  (aqueous) (68%); (ii)  $\text{CH}_2\text{N}_2$ ,  $\text{Et}_2\text{O}$  (91%); (iii)  $\text{DBU}$ ,  $\text{CHCl}_3$  (100%); (iv)  $\text{LiOH}$ ,  $\text{THF-H}_2\text{O}$  (72%).

Scheme II<sup>a</sup>

<sup>a</sup> (i)  $\text{NaH}$ ,  $(\text{MeO})_2\text{CO}$ ,  $\text{C}_6\text{H}_6$  (86%); (ii)  $\text{Br}_2$ ,  $\text{Et}_2\text{O}$ ; (iii)  $\text{NaOMe}$ ,  $\text{MeOH}$  (37% from 8); (iv)  $\text{DIBALH-}n\text{-BuLi}$ ,  $\text{hexane-THF}$ ,  $-78^\circ\text{C}$   $\rightarrow$  room temperature (62%).

Scheme III<sup>a</sup>

<sup>a</sup> (i)  $\text{DCC}$ ,  $\text{DMAP}$ ,  $\text{DMAP-HCl}$ ,  $\text{CHCl}_3$ ,  $\Delta$ , 20 h (51%); (ii)  $h\nu$ ,  $\text{CH}_2\text{Cl}_2$ , 4 h (63%); (iii) toluene,  $\Delta$ , 2 h (100%); (iv)  $\text{LiOH}$ ,  $\text{H}_2\text{O}$ -dioxane; (v)  $\text{KMnO}_4$ , then  $\text{HCl}$  (aqueous) (37% from 17).

to give the more stable *cis* isomer **1**. The synthetic material was identical with a sample of natural byssochlamic acid by comparison of IR,  $^1\text{H}$  and  $^{13}\text{C}$  NMR, and mass spectra.

**Acknowledgment.** We are indebted to Professor D. H. R. Barton for a sample of natural byssochlamic acid, to Dr. Steven T. Perri for preliminary work, and to Rodger L. Kohnert for valuable technical assistance with NMR studies. Financial support was provided by the National Science Foundation (CHE-9015466). R.J.B. thanks the Council for International Exchange

of Scholars for a Fulbright travel grant.

**Supplementary Material Available:** Spectral and analytical data for compounds **3-6**, **8-17**, and **1** (4 pages). Ordering information is given on any current masthead page.

An Empirical Correlation between  $^1J_{\text{C}_\alpha\text{H}_\alpha}$  and Protein Backbone Conformation

Geerten W. Vuister, Frank Delaglio, and Ad Bax\*

Laboratory of Chemical Physics  
National Institute of Diabetes and Digestive and  
Kidney Diseases, National Institutes of Health  
Bethesda, Maryland 20892

Received April 14, 1992

Determination of the solution structure of a protein by NMR relies primarily on the analysis of a large number of  $^1\text{H}$ - $^1\text{H}$  NOE interactions, supplemented by dihedral angle information derived from vicinal  $^1\text{H}$ - $^1\text{H}$   $J$  couplings. Three-bond couplings are commonly interpreted in terms of dihedral angles using the well-known Karplus relationship and can provide information on the backbone angle  $\phi$  and the side-chain torsion angles  $\chi_n$ . In principle,  $^3J_{\text{H}_\alpha\text{N}}$  couplings can be used to extract information about the backbone angle  $\psi$ , but in practice the variation in  $^3J_{\text{H}_\alpha\text{N}}$  as a function of  $\psi$  is too small for this purpose.<sup>1</sup> The correlation between the magnitude of  $^1J_{\text{C}_\alpha\text{H}_\alpha}$  and the backbone angles  $\phi$  and  $\psi$  has been investigated previously both by MO calculations and by experimental measurements on conformationally constrained cyclic peptides.<sup>2</sup> From this work, it was concluded that the magnitude of  $^1J_{\text{C}_\alpha\text{H}_\alpha}$  is influenced primarily by the interaction between the  $\text{H-C}_\alpha$  bonding orbital and the  $p_z$  orbital of the lone pair N electrons; i.e.,  $^1J_{\text{C}_\alpha\text{H}_\alpha}$  was expected to depend primarily on  $\phi$ .<sup>3</sup> Here we present experimental results that indicate that  $^1J_{\text{C}_\alpha\text{H}_\alpha}$  is determined primarily by  $\psi$  and to a lesser extent by  $\phi$ .

$^1J_{\text{C}_\alpha\text{H}_\alpha}$  couplings have been measured for the proteins basic pancreatic trypsin inhibitor (BPTI), staphylococcal nuclease (SNase), and calmodulin (CaM). Previous NMR studies have indicated that the solution structures of these proteins for residues 3-56 (BPTI), 8-42 and 55-140 (SNase), and 6-76 and 83-146 (CaM) are in good agreement with the crystal structures.<sup>4-6</sup> In the present work, we correlate the magnitude of  $^1J_{\text{C}_\alpha\text{H}_\alpha}$  with dihedral angles obtained from the X-ray crystal structures.<sup>7-9</sup>  $^1J_{\text{C}_\alpha\text{H}_\alpha}$  values were measured from the  $F_2$  splittings in the purged<sup>10</sup> HMQC spectrum of natural abundance BPTI (11 mM,  $p^2\text{H}$  5.8) and from the antiphase  $F_3$  splittings in the 3D CT-HCACO<sup>11</sup> and HCCH-COSY<sup>12</sup> spectra of uniformly (>95%)  $^{13}\text{C}$ -enriched SNase

(1) Kopple, K. D.; Ahsan, A.; Barfield, M. *Tetrahedron Lett.* **1978**, *38*, 3519-3522.

(2) Egli, H.; von Philipsborn, W. *Helv. Chim. Acta* **1981**, *64*, 976-988.

(3) Gil, V. M. S.; von Philipsborn, W. *Magn. Reson. Chem.* **1989**, *27*, 409-430.

(4) Wagner, G.; Braun, W.; Havel, T. F.; Schaumann, T.; Go, N.; Wüthrich, K. *J. Mol. Biol.* **1987**, *196*, 611-639.

(5) Ikura, M.; Spera, S.; Barbato, G.; Kay, L. E.; Krinks, M.; Bax, A. *Biochemistry* **1991**, *30*, 9216-9228.

(6) Torchia, D. A.; Sparks, S. W.; Bax, A. *Biochemistry* **1989**, *28*, 5509-5524.

(7) Wlodawer, A.; Deisenhofer, J.; Huber, R. *J. Mol. Biol.* **1987**, *193*, 145-156.

(8) Loll, P. J.; Lattman, E. E. *Proteins: Struct., Funct., Genet.* **1989**, *5*, 183-201.

(9) Babu, Y. S.; Bugg, C. E.; Cook, W. I. *J. Mol. Biol.* **1988**, *204*, 191-204.

(10) Sørensen, O. W.; Ernst, R. R. *J. Magn. Reson.* **1983**, *51*, 477-489.

(11) Powers, R.; Gronenborn, A. M.; Clore, G. M.; Bax, A. *J. Magn. Reson.* **1991**, *94*, 290-213.

(12) Bax, A.; Gronenborn, A. M.; Clore, G. M. *J. Magn. Reson.* **1990**, *88*, 425-431.

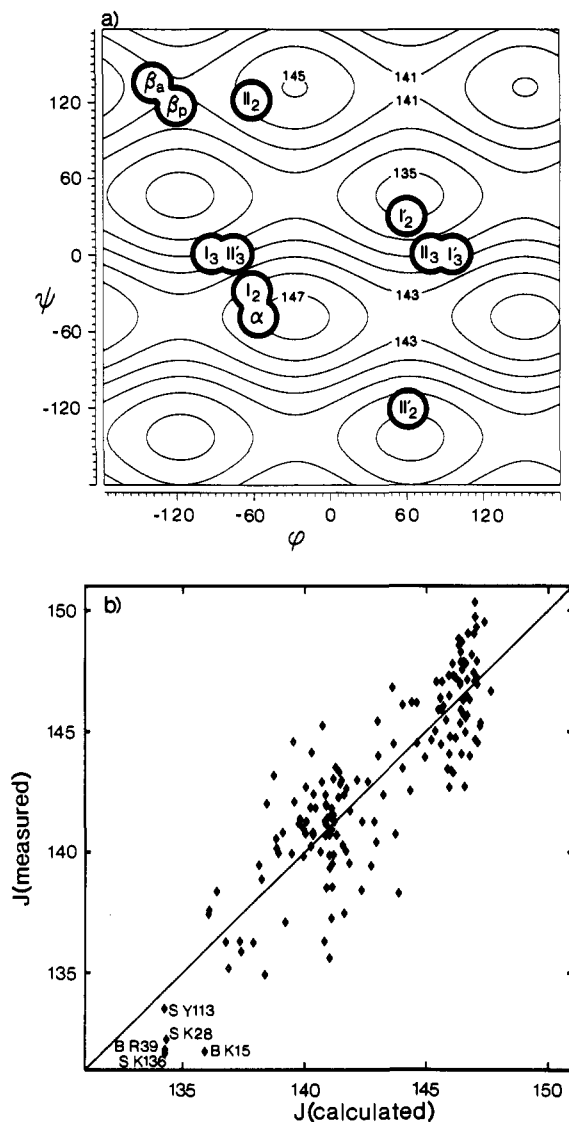


**Figure 1.** (a) Contour plot of eq 2. The average backbone angles for residues in  $\alpha$ -helical and parallel and antiparallel  $\beta$ -sheets are marked as  $\alpha$ ,  $\beta_p$ , and  $\beta_n$ , respectively. The second and third residues in a type X turn ( $X = I, Y, II$ , or  $II'$ ) are marked  $X_2$  and  $X_3$ . (b)  $^1J_{CaHa}$  couplings calculated from the crystal structures of BPTI, SNase, and CaM using eq 2 versus the values observed in the previously assigned NMR spectra.<sup>16-18</sup> Residues with  $^1J_{CaHa} < 134$  Hz are marked (B: BPTI; S: SNase).

(1.5 mM,  $p^2H$  6.5) and CaM (1.0 mM,  $p^2H$  6.8); all were recorded without  $^{13}C$  decoupling during data acquisition. In addition, for SNase and CaM  $^1J_{CaHa}$  values were also measured from pseudo-3D,  $J$ -resolved experiments to be described elsewhere. Both CaM and SNase were enriched uniformly with  $^{13}C$  and  $^{15}N$ . All spectra were recorded at 600.14 MHz ( $^1H$  frequency) on a Bruker AMX600 operating at 35 °C. Glycines and prolines were excluded from the database. Typical data are shown in the supplementary material. Precise measurements of  $^1J_{CaHa}$  were made for 162 residues, and these data, together with the crystallographically determined backbone angles  $\phi$  and  $\psi$ , are reported in the supplementary material.

Theoretical considerations suggest a positive contribution to  $^1J_{CaHa}$  originating from the adjacent  $p_z$  nitrogen orbital and a negative contribution due to the antibonding  $\pi$  orbital of the carbonyl group. An equation describing the  $^1J_{CaHa}$  dependence on  $\phi, \psi$  of the form

$$J = A + B \cos 2(\psi + 150^\circ) + C \cos 2(\phi + 30^\circ) \quad (1)$$

was suggested previously.<sup>2,3</sup> However, best fit procedures using singular-value decomposition indicated that this equation did not

yield an adequate fit. Indeed, it may be expected that interaction between the carbonyl  $\pi$  orbital and the  $C_\alpha-H_\alpha$  bonding orbital is not invariant to  $180^\circ \psi$  rotations, and an additional term,  $\sin(\psi + 150^\circ)$ , is needed to account for this asymmetry. Statistical analysis of the best fit with this extended form of eq 1 indicates that the fit is not satisfactory, and an additional  $-12^\circ$  empirical "phase shift" is needed to properly account for the  $\phi, \psi$  dependence of the measured data.<sup>13</sup> A good description of the experimental data is then obtained with

$$^1J_{CaHa} = 140.3 + 1.4 \sin(\psi + 138^\circ) - 4.1 \cos 2(\psi + 138^\circ) + 2.0 \cos 2(\phi + 30^\circ) \quad (2)$$

Inclusion of additional trigonometric terms in eq 2 did not yield statistically significantly better fits. Figure 1a shows a contour map of eq 2 as a function of  $\phi$  and  $\psi$ . Figure 1b shows the comparison of the couplings calculated using eq 2 with the observed NMR values, showing good agreement with an RMS difference of 2.0 Hz. This residual is significantly larger than the estimated error ( $\sim 1$  Hz)<sup>14</sup> in our measurement of  $^1J_{CaHa}$ . However, our analysis does not account for different substituents at the  $C_\beta$  position, which possibly could have a significant effect on  $^1J_{CaHa}$ . Also, one-bond  $J$  couplings are known to be influenced by electric fields.<sup>15</sup> The present protein  $J$  coupling data, together with the high-resolution crystal structure, permit a detailed re-investigation of the importance of these effects.

Residues in an extended  $\beta$ -sheet conformation on average have relatively small  $^1J_{CaHa}$  values ( $140.5 \pm 1.8$  Hz), whereas significantly larger values ( $146.5 \pm 1.8$  Hz) are found for  $\alpha$ -helical residues. In this respect it is interesting to note that the four residues, Asp78-Ser 81, in the middle of the "central helix" of calmodulin have  $^1J_{CaHa}$  couplings (142.7, 141.8, 143.4, and 142.9 Hz) close to their random coil values and significantly smaller than the values that would be expected on the basis of the  $\phi, \psi$  angles of the crystal structure. This confirms conclusions from a recent  $^{15}N$  relaxation study that indicated high flexibility for these residues in solution.<sup>16</sup>

All four non-glycine residues with positive  $\phi$  angles in our database exhibit unusually small values ( $< 134$  Hz) and have been marked in Figure 1b. The only other residue with  $^1J_{CaHa} < 134$  Hz is Lys15 in BPTI ( $^1J_{CaHa} = 131.8$  Hz), which has a value that is 4 Hz smaller than that expected on the basis of eq 2. Identification of residues with positive  $\phi$  angles can sometimes be difficult, and  $^1J_{CaHa}$  may serve as a useful additional marker for identifying such residues.

**Acknowledgment.** We thank Dennis Torchia for providing us with the  $^{13}C$ -enriched SNase sample and its  $^{13}C$  resonance assignments and Michael Barfield for useful discussions. This work was supported by the AIDS Targeted Anti-Viral Program of the Office of the Director of the National Institutes of Health. G.W.V. acknowledges financial support from the Netherlands Organization of Scientific Research (NWO).

**Registry No.** BPTI, 9087-70-1; SNase, 9013-53-0.

**Supplementary Material Available:** A table containing 162  $^1J_{CaHa}$  couplings together with the  $\phi$  and  $\psi$  angles obtained from crystallographic data and figures showing cross sections through the 3D data sets, from which  $^1J_{CaHa}$  values were obtained (7 pages). Ordering information is given on any current masthead page.

(13) A statistical  $F$ -test shows that inclusion of the additional phase shift in eq 2 is significant at the 0.1% confidence level: Draper, N. R.; Smith, H. *Applied Regression Analysis*, 2nd ed.; Wiley: New York, 1981.

(14)  $J$  couplings obtained from the CT-HSQC  $J$ -modulated 2D CT-HSQC experiment and values obtained from the 3D CT-HACO experiment show root-mean-square differences of 1.05 Hz (CaM) ( $n = 57$ ) and 0.92 Hz (SNase) ( $n = 74$ ).

(15) Barfield, M.; Johnston, M. D., Jr. *Chem. Rev.* **1973**, *73*, 53-73.  
(16) Barbato, G.; Ikura, M.; Kay, L. E.; Bax, A. *Biochemistry* **1992**, *31*, 5269-5278.

(17) Wagner, G.; Bruehwiler, D. *Biochemistry* **1986**, *25*, 5939-5843.  
(18) Baldisseri, D. M.; Torchia, D. A. Private communication.  
(19) Ikura, M.; Kay, L. E.; Bax, A. *Biochemistry* **1990**, *29*, 4659-4667.